Targeting Cancer Cells: Controlling the Binding and Internalization of Antibody-Functionalized Capsules

Angus P. R. Johnston,[†,*] Marloes M. J. Kamphuis,[†] Georgina K. Such,[†] Andrew M. Scott,[‡] Edouard C. Nice,[§,⊥] Joan K. Heath,[§] and Frank Caruso[†,*]

[†]Department of Chemical and Biomolecular Engineering, The University of Melbourne, Victoria 3010, Australia, [‡]Ludwig Institute for Cancer Research, Austin Hospital, Victoria 3084, Australia, [§]Ludwig Institute for Cancer Research, Royal Melbourne Hospital, Parkville, Victoria 3050, Australia, and [⊥]Department of Biochemistry and Molecular Biology, Monash University, Victoria 3800, Australia

ABSTRACT The development of nanoengineered particles, such as polymersomes, liposomes, and polymer capsules, has the potential to offer significant advances in vaccine and cancer therapy. However, the effectiveness of these carriers has the potential to be greatly improved if they can be specifically delivered to target cells. We describe a general method for functionalizing nanoengineered polymer capsules with antibodies using click chemistry and investigate their interaction with cancer cells *in vitro*. The binding efficiency to cells was found to be dependent on both the capsule-to-cell ratio and the density of antibody on the capsule surface. In mixed cell populations, more than 90% of target cells bound capsules when the capsule-to-target cell ratio was 1:1. Strikingly, greater than 50% of target cells exhibited capsules on the cell surface even when the target cells were present as less than 0.1% of the total cell population. Imaging flow cytometry was used to quantify the internalization of the capsules, and the target cells were found to internalize capsules efficiently. However, the role of the antibody in this process was determined to enhance accumulation of capsules on the cell surface rather than promote endocytosis. This represents a significant finding, as this is the first study into the role antibodies play in internalization of such capsules. It also opens up the possibility of targeting these capsules to cancer cells using targeting molecules that do not trigger an endocytic pathway. We envisage that this approach will be generally applicable to the specific targeting of a variety of nanoengineered materials to cells.

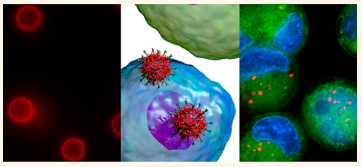

KEYWORDS: drug delivery · antibodies · cell targeting · layer-by-layer · click chemistry · internalization · nanoparticle

The targeted delivery of drugs to specific cells has the potential to achieve therapeutically relevant doses at the site of action while minimizing potentially harmful side effects.[1−3] The development of therapeutic carriers that can deliver high payloads, while protecting the encapsulated drug from degradation, is currently of significant interest. Critical to targeted delivery is the ability to develop and functionalize drug delivery vehicles that exhibit low nonspecific binding to cells using specific targeting molecules, such as antibodies, ligands, and mimetics.[4,5] This can be achieved *via* a number of methods, including carbodiimide, thiol/maleimide, and biotin/avidin coupling chemistries.[6] While these techniques have been applied previously for a number of applications,[6] there is an urgent need for coupling reactions that are stable in mild, aqueous conditions that do not undergo unwanted side reactions and preserve the activity of the delicate targeting molecules.

An emerging coupling strategy is click chemistry, chiefly the Cu(I)-catalyzed azide−alkyne Huisgen cycloaddition reaction (CuAAC), which proceeds rapidly in mild aqueous conditions, undergoes negligible unwanted side reactions, and where the reactants are stable and largely unreactive until the addition of the Cu(I) catalyst.[7] Click chemistry has been used to couple a number of small targeting molecules, such as folate[8] and RGD peptides, to a variety of surfaces.[9,10] However, until recently, the use of CuAAC click chemistry to conjugate whole antibodies (Abs) to surfaces has been limited.[11−13] This is principally due to the presence of Cu(I), which can trigger irreversible aggregation of the Ab.[11] Recently, we developed a method to couple azide-functionalized Abs to alkyne-modified capsules using a chelated Cu(I) catalyst (Scheme 1 and Figure S1 in the Supporting Information) and demonstrated specific targeting to cancer cells, even when the target population is present as less than 0.1% of the total cell population.[11] Herein, we present a detailed investigation of the factors that influence the binding and internalization of such Ab-functionalized capsules to cancer cells. In this study, we have explored the role of (i) the capsule-to-cell ratio, (ii) the

* Address correspondence to angusj@unimelb.edu.au; fcaruso@unimelb.edu.au.

Received for review March 9, 2012 and accepted July 24, 2012.

Published online August 07, 2012
10.1021/nn3010476

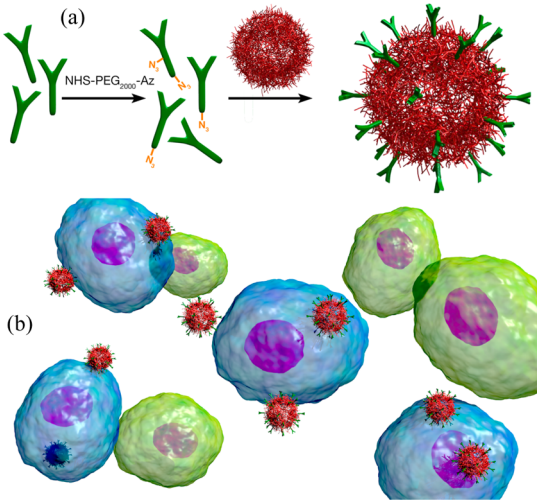

Scheme 1. (a) Click functionalization of LbL capsules using an azide-modified antibody. (b) Humanized A33 mAb_{Az}-functionalized capsules are added to a mixed population of cells that either express the complementary antigen (LIM2405+, blue) or do not express the complementary antigen (LIM2405−, green).

density of the Ab on the surface of the capsules, (iii) the percentage of target cells in a mixed cell population, and (iv) the type of Ab, on the binding and internalization of capsules by the cells.

The capsules used in this study were generated by layer-by-layer (LbL) deposition of alkyne-modified poly(*N*-vinylpyrrolidone) ($PVPON_{Alk}$) and poly(methacrylic acid) (PMA) on 585 nm diameter silica spheres.[14] Assembly was performed at pH 4, where there is strong hydrogen bonding between the protonated carboxylic acid of PMA and the carbonyl oxygen of PVPON. Above the pK_a of PMA (pH ~6.5), the hydrogen bonding between PMA and PVPON is disrupted and the capsules disassemble. To impart stability at physiological conditions (pH 7.4), the alkyne groups on the $PVPON_{Alk}$ were cross-linked with a bifunctional poly(ethylene glycol) (PEG) azide.[14] This linker also contains a redox cleavable disulfide group that can degrade in simulated reducing conditions of the cellular cytoplasm.[15] After cross-linking and removal of the silica core with buffered hydrofluoric acid (HF), the capsules were placed in phosphate buffered saline (PBS) at pH 7, where the hydrogen bonding interaction between PMA and PVPON is disrupted, causing the PMA to be expelled from the film (during this process, the capsules swell to be approximately 800 nm in diameter[14]). This generates capsules formed exclusively from the low fouling polymer PVPON, held together with biologically cleavable disulfide bonds. Previously, we demonstrated that sufficient alkyne groups remain for subsequent functionalization of the film.[11,14] While the work presented here focuses on the functionalization of capsules prepared using the LbL process, the general nature of click chemistry means that this approach is applicable to a variety of delivery techniques, including liposomes, micelles, polymersomes, and polyion complexes.[1,16]

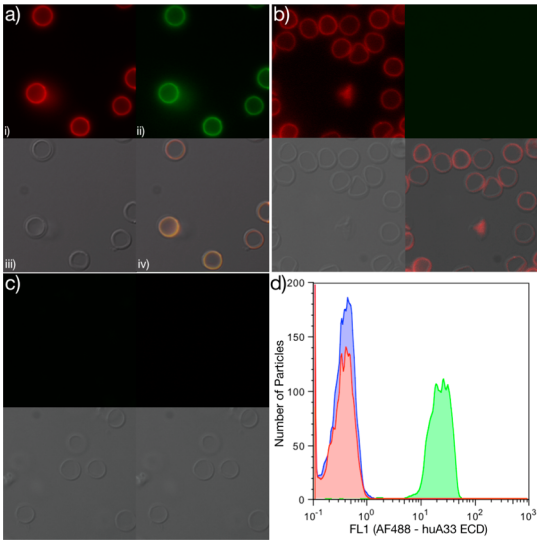

Figure 1. Fluorescence microscopy images of huA33 mAb_{Az}-functionalized $PVPON_{Alk}$ capsules. Capsules incubated with (a) huA33 mAb in the presence of Cu(I) and chelator, (b) IgG in the presence of Cu(I) and chelator, and (c) huA33 mAb_{Az} in the absence of Cu(I) and chelator. (i) Antibody (huA33 mAb_{Az} in a and c, IgG in b) was labeled with AF647 (red), (ii) AF488-labeled hA33 extracellular domain (ECD; antigen for huA33 mAb) (green), (iii) bright-field, and (iv) overlay images. (d) Flow cytometry histogram of the binding of AF488-labeled hA33 ECD to huA33 mAb_{Az}-functionalized capsules (green profile), IgG-functionalized capsules (red profile), and capsules incubated with huA33 without Cu(I) or chelator (blue profile).

The Ab chosen for this study was the humanized A33 monoclonal antibody (huA33 mAb), which has attracted considerable clinical attention for the targeting of colorectal cancer (CRC).[17] Greater than 95% of primary and metastatic colorectal cancers express the A33 antigen,[17] and in various clinical trials A33 mAbs have been shown to localize specifically to human primary and metastatic CRC cells. Apart from its expression by normal intestinal and pyloric gastric epithelia, the A33 antigen exhibits very low or negligible expression by other tissues.[18] To attach the huA33 mAb to the capsules using click chemistry, it first needs to be modified with azide groups. This may be achieved either in a site-specific manner, where the mAb is engineered to contain a C-terminal thioester that is reactive to a click-modified peptide containing an N-terminal cysteine,[12] or by using amine succinimidyl ester coupling chemistry. We previously demonstrated azide (Az) modification of the huA33 mAb by reacting it with a linear, bifunctional PEG that has a succinimidyl ester group at one end (reactive toward lysine) and an azide at the other (NHS-PEG2000-Az). The majority of the lysine residues (~65%) in huA33 mAb are located in the Fc portion, so statistically, the functionalization should occur preferentially in the Fc portion.[17] Using a 10-fold excess of NHS-PEG2000-Az, an average of one azide group was attached to the antibody, as determined by MALDI.[11] Broadening of the peak in the MALDI

spectrum indicated that there was a range of functionalization, from 0 to 2 PEG_{Az} molecules per Ab.

The Ab-functionalized capsules developed in this study, along with an understanding of how they interact with CRC cells, is likely to have significant implications for the development of carriers for cancer therapy, vaccines, and gene therapy.

RESULTS AND DISCUSSION

Capsule Functionalization. We have previously demonstrated the functionalization of capsules with Ab using AlexaFluor 647 (AF647)-labeled huA33 mAb_{Az} and IgG_{Az}.[11] To gain a better understanding of the activity and specificity of the immobilized Abs, we probed the antigen binding using an AF488-labeled recombinant fragment (the extracellular domain [ECD]) of the human A33 antigen (hA33). Capsules of ~3.8 μm in diameter were used for this part of the study to facilitate flow cytometry analysis, as the sub-micrometer-sized capsules (~800 nm) used for the cell binding and internalization experiments are too small to individually analyze using conventional flow cytometry. The use of larger capsules also enabled microscopy images to be taken with sufficient resolution. Both huA33 mAb_{Az} and IgG_{Az} were clicked onto the surface of the capsules, as evidenced by the red fluorescence of the capsules (Figure 1a,b). No fluorescence was detected for capsules incubated with huA33 mAb_{Az} in the absence of the Cu(I) catalyst and chelator (Figure 1c).

The specificity of the immobilized Abs was demonstrated by incubating the functionalized capsules with the AF488-labeled hA33 ECD. As anticipated, the ECD bound specifically to the huA33 mAb_{Az}-functionalized capsules but not to IgG-functionalized capsules (Figure 1a,b). Similarly, the capsules incubated with huA33 mAb_{Az}, but without the Cu(I) catalyst, did not show significant ECD binding (Figure 1c). These results were confirmed by flow cytometry (Figure 1d), which showed that huA33 mAb_{Az}-functionalized capsules incubated with hA33 ECD exhibited an average fluorescence intensity of 21.5 au, compared with 0.28 au for IgG-functionalized capsules and 0.35 au for capsules incubated with huA33 mAb_{Az} without Cu(I) catalyst.

Determining the exact amount of Ab immobilized onto the surface of the capsules is challenging, as cross-reactivity between the polymer and Cu(I) with standard *in situ* protein quantification reagents (*e.g.*, microBCA or NanoOrange) interferes with the measurements. In our experiments, Cu(I) is unlikely to have a significant effect on cell viability, as recent studies have shown that chelated Cu(I) has minimal cellular toxicity.[19] We therefore immobilized AF488-huA33 mAb_{Az} and, after functionalization, degraded the capsules with 1 mg mL^{-1} dithiothreitol (DTT). This overcomes any issues associated with Ab fluorescence quenching, which is likely to occur when the Abs are conjugated to the capsules at high concentration. When 20 μg of huA33 mAb_{Az} was incubated with 1.6×10^6 capsules, approximately $(9 \pm 2) \times 10^4$ Abs per capsule were immobilized (Figures S2 and S3), corresponding to a surface area of ~23 nm^2 per Ab (assuming a hard sphere model for the 800 nm diameter capsules). This agrees well with our previously reported density determined using the difference method (~$(7 \pm 4) \times 10^4$ Abs per capsule).[11] The surface footprint of the Y-shaped IgG molecule is between 14 and 32 nm^2, suggesting a high density layer of Ab on the surface of the capsule. It is also likely the Abs penetrate into the LbL film, leading to greater than monolayer density of Ab. This high density Ab coverage ensures that if a capsule comes in contact with a cell, there is an opportunity for the Ab to bind to a cell surface receptor, regardless of the orientation of the capsule. If the Ab density is too low, when a capsule comes in contact with the cell, there may be no Abs in the correct orientation to facilitate capsule binding.

Cell Targeting. The specific binding of huA33 mAb_{Az}-functionalized capsules was investigated using AF647-labeled capsules incubated with the LIM1899 CRC cell line,[20] which expresses the A33 antigen on the cell surface.[21] Capsule binding was performed at 4 °C for 1 h to eliminate variations that could be caused by internalization of the capsules. All experiments were performed in triplicate on the same day as variations in the cell density, deposition of extracellular matrix, and passage number can affect the degree of capsule binding to cells. To determine the optimal concentration for targeting the cancer cells, the capsule-to-cell ratio was varied from 10:1 to 600:1 (Figure 2a). Nonfunctionalized capsules and IgG_{Az}-functionalized capsules showed a similar level of nonspecific binding, which increased linearly to around 12% of cells at a 600:1 capsule-to-cell ratio. For huA33 mAb_{Az}-functionalized capsules, the percentage of cells with capsules bound increased rapidly as the ratio was increased from 10:1 to 100:1. At a 100:1 capsule-to-cell ratio, more than 85% of the cells had huA33 mAb_{Az}-functionalized capsules bound. In contrast, only ~5% of the cells incubated with the IgG_{Az}-functionalized and nonfunctionalized capsules had capsules bound. A slight increase in the percentage of cells with capsules bound was observed when the capsule-to-cell ratio was further increased to 600:1. However, as shown by the flow cytometry histograms (Figure 2b,c), the average fluorescence intensity of the cells increased as the capsule-to-cell ratio increased, thereby indicating, as expected, that the number of capsules per cell increased as the capsule-to-cell ratio was increased. Conventional flow cytometry does not allow for the direct quantification of the number of capsules bound per cell; however, this can be achieved using imaging flow cytometry (see section on Internalization of Capsules into Cancer Cells). There was no significant increase in the nonspecific binding of IgG_{Az}-functionalized and nonfunctionalized capsules to the LIM1899 cells as the capsule-to-cell ratio increased.

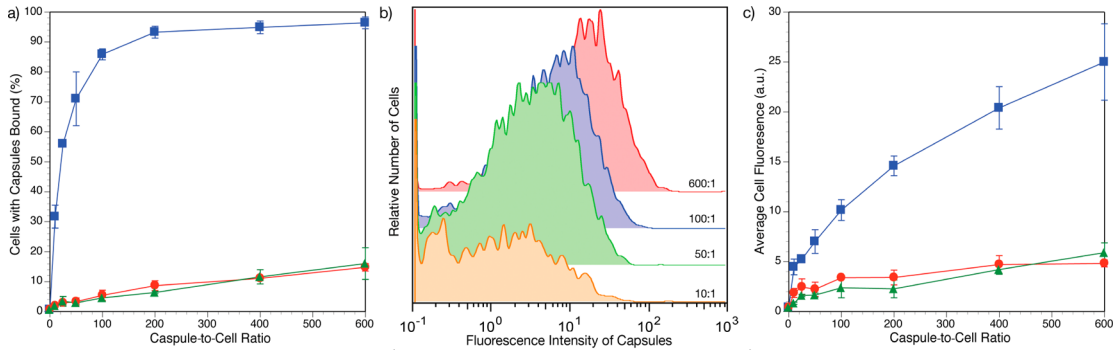

Figure 2. Effect of capsule/cell ratio on the binding of $PVPON_{Alk}$ capsules to LIM1899 CRC cells. Flow cytometry analysis was performed after cells were incubated with capsules at 4 °C for 1 h. Each capsule was functionalized with an average of 9×10^4 Ab, and the capsule-to-cell ratio was varied from 10:1 to 600:1. (a) Percentage of cells with capsules bound (huA33 mAb_{Az}-functionalized capsules, blue squares; IgG-functionalized capsules, red circles; nonfunctionalized capsules, green triangles). (b) Flow cytometry histograms showing huA33 mAb_{Az}-functionalized capsule binding at different capsule/cell ratios. (c) Mean fluorescence intensity of cells with capsules associated (huA33 mAb_{Az}-functionalized capsules, blue squares; IgG-functionalized capsules, red circles; nonfunctionalized capsules, green triangles).

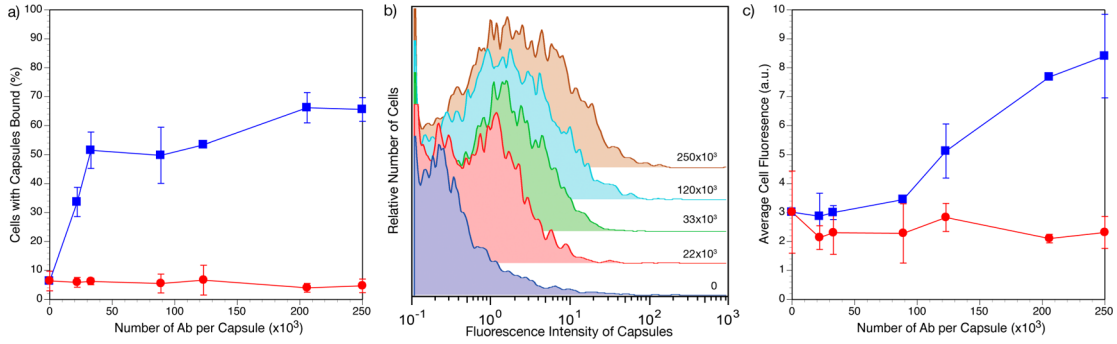

Figure 3. Effect of Ab density on the binding of $PVPON_{Alk}$ capsules to LIM1899 cells. Flow cytometry analysis was performed after the cells were incubated with capsules at a 100:1 capsule-to-cell ratio at 4 °C for 1 h. (a) Percentage of cells with capsules bound (huA33 capsules, blue squares; IgG capsules, red circles). (b) Flow cytometry histograms showing huA33 mAb_{Az}-functionalized capsule binding with increasing Ab density. (c) Mean fluorescence intensity of cells associated with capsules (huA33 capsules, blue squares; IgG capsules, red circles).

The degree of huA33 mAb_{Az} functionalization was also investigated to determine the effect on capsule binding. The capsule-to-cell ratio was fixed at 100:1 and the number of huA33 mAb_{Az} per capsule was varied from 2×10^4 to 2.5×10^5. An increase in the percentage of cells with capsules bound was observed from ~35% of cells with 2×10^4 of huA33 mAb_{Az} per capsule to ~60% with 2.5×10^5 of huA33 mAb_{Az} per capsule (Figure 3a). This value was somewhat lower than that observed in Figure 2 and is likely due to the variability observed in the culturing of the LIM1899 cells (Figure S4). While the trends observed for these cells were consistent from day to day, the absolute values for the capsule binding varied by up to 20%. For this reason, experiments were performed in triplicate on the same day. There was no impact on the degree of nonspecific binding as the amount of IgG_{Az} was increased. Interestingly, the fluorescence intensity of the cells, reflecting the number of capsules bound per cell, also increased as the density of the huA33 mAb_{Az} on the capsule surface increased (Figure 3b,c). The average fluorescence intensity of cells with capsules bound doubled when the number of huA33 $mAbs_{Az}$ was increased from 9×10^4 to 2×10^5 per capsule. This indicates that the higher packing density of huA33 mAbs on the surface of the capsule promotes capsule binding. Again, increasing the IgG_{Az} concentration did not affect the number of capsules bound to cells.

Deconvolution microscopy was used to confirm the binding of huA33 mAb_{Az}-functionalized capsules to LIM1899 cells (Figure 4a). Once again, nonfunctionalized (not shown) and IgG-functionalized capsules (Figure 4b) showed limited nonspecific binding.

Targeting Subpopulations of Cancer Cells. In an *in vivo* setting, cancer cells, whether they are propagating within an organ or suspended in circulation, represent only a small proportion of the cells in their immediate vicinity. This is particularly true for small deposits of metastatic cancer cells that have only recently taken up residence in a secondary organ. To assess the ability of huA33 mAb_{Az}-functionalized capsules to specifically target cancer cells in a mixed population, where a proportion of cells express the hA33 antigen and a proportion do not, we exploited the LIM2405 CRC cell line.[21] While native LIM2405 cells do not express the A33 antigen, a stably transfected clonal cell line expressing

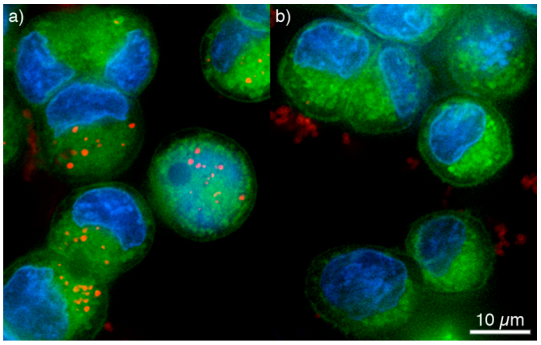

Figure 4. Deconvolution microscopy images of (a) huA33- or (b) IgG-functionalized $PVPON_{Alk}$ capsules incubated with LIM1899 CRC cells at 37 °C for 24 h. Capsules are labeled with AF647 (red), cells are labeled with LavaCell (fake colored green), and the nucleus is labeled with Hoechst 33342 (blue).

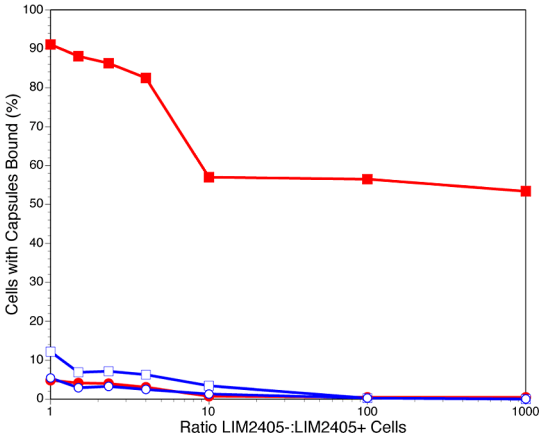

Figure 5. Flow cytometry analysis of the binding of $PVPON_{Alk}$ capsules to a mixed population of LIM2405+ (squares) and LIM2405− (circles) CRC cells at 4 °C for 1 h; huA33- (red, solid symbols) and IgG-functionalized capsules (blue, hollow symbols).

recombinant hA33 antigen has been created (LIM2405+).[11] A clonal LIM2405 cell line (LIM2405−) harboring the control (empty) expression vector provides a suitable control. This cell system enables the specific binding of huA33 mAb_{Az}-functionalized capsules to be studied in detail in the absence of variation in nonspecific binding that can occur when using different cell types that express different surface proteins. To track the different cell populations, LIM2405+ cells were labeled with CellTracker CMFDA and LIM2405− cells were labeled with LavaCell. The capsule-to-LIM2405+ cell ratio was kept constant at 100:1 in all experiments.

As we reported previously, greater than 90% of LIM2405+ cells bound huA33 mAb_{Az}-functionalized capsules in a 50:50 mixture of LIM2405+/LIM2405− cells.[11] In contrast, less than 5% of LIM2405− cells bound capsules.[11] IgG_{Az}-functionalized capsules showed low levels (<10%) of nonspecific binding to both cell types. A higher degree of nonspecific binding was observed for the LIM2405+ cells compared to the LIM2405− cells. This suggests the presence of the A33 molecule on the surface of the cell makes the cells more "adherent" and increases nonspecific binding. In the current study, we demonstrate that when the proportion of LIM2405− cells is increased to a 4-fold excess over the LIM2405+ cells, the percentage of LIM2405+ cells with huA33 mAb_{Az}-functionalized capsules bound remains at >80% (Figure 5). Indeed, even when the LIM2405−/LIM2405+ cell ratio is increased to 10:1, 100:1, and 1000:1, more than 55% of the LIM2405+ cells bound huA33 mAb_{Az}-functionalized capsules, while nonspecific binding remains at less than 5%. This is potentially a significant result in a therapeutic context, as it demonstrates the ability to target a very small population of cells within a milieu of cells. While a 100:1 ratio of capsules-to-target cells is required to give optimal targeting, the number of cells to be targeted can be very low. This result suggests that targeted antibody therapies are likely to have impact in an adjuvant setting after the surgical removal of the primary tumor. Here the challenge is to kill undetectable deposits of metastatic cells (micrometastases) that have lodged in an organ distant from the primary tumor. While *in vivo* targeting of micrometastases is dependent on a number of additional factors, including blood circulation time of the capsules, and the vascularization, extravasation, and penetration of the micrometastases, our data indicate that the capsule targeting system described here may have potential use in such settings[1] and warrants further investigation.

Internalization of Capsules into Cancer Cells. Critical to delivering drugs to cancer cells is the efficient internalization of the capsules. To evaluate the cellular internalization of the capsules, separate populations of LIM2405+ and LIM2405− cells were incubated with the huA33 mAb_{Az}-, IgG-, and nonfunctionalized capsules at 37 °C for 2 h. The huA33 mAb_{Az}-functionalized capsules were also incubated with LIM2405+ capsules at 4 °C for 2 h to provide a control for noninternalized capsules. To permit robust statistical analysis, imaging flow cytometry was used to study the internalization of the capsules (Figures 6 and 7a−c). The imaging flow cytometer acquires a cross-sectional image of each cell, approximately 2 μm deep. Accordingly, it is important to note that the readout does not correspond to the total number of capsules that have been internalized by the cells. Rather, it provides a comparison of the number of capsules in a fixed cross-sectional volume of the cells. Using this approach, we found that 45% of the LIM2405+ cells incubated with huA33 mAb_{Az}-functionalized capsules contained internalized capsules. By comparison, less than 5% of LIM2405− cells and LIM2405+ cells incubated with IgG-functionalized capsules contained internalized capsules (Figure 6a). We counted the number of spots associated with each cell using the IDEAS software and assumed that each spot corresponds to 1 capsule. However, it is possible that some spots correspond to

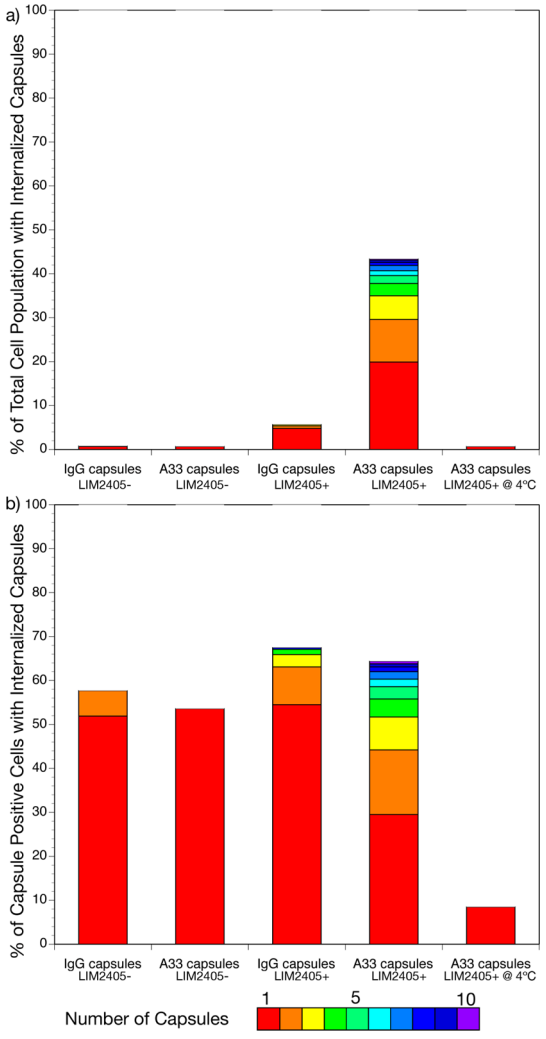

Figure 6. Role of Ab functionalization in the internalization of capsules into LIM2405+ and LIM2405− cells. Cells were incubated with capsules at 37 °C for 2 h, unless otherwise indicated, and the number of capsules internalized by the cells was determined using imaging flow cytometry. (a) Percentage of the total cell population with internalized capsules. (b) Analysis of internalization by cells with capsules bound. The color of the histogram corresponds to the number of capsules inside the cell, ranging from 1 (red) to more than 10 (violet).

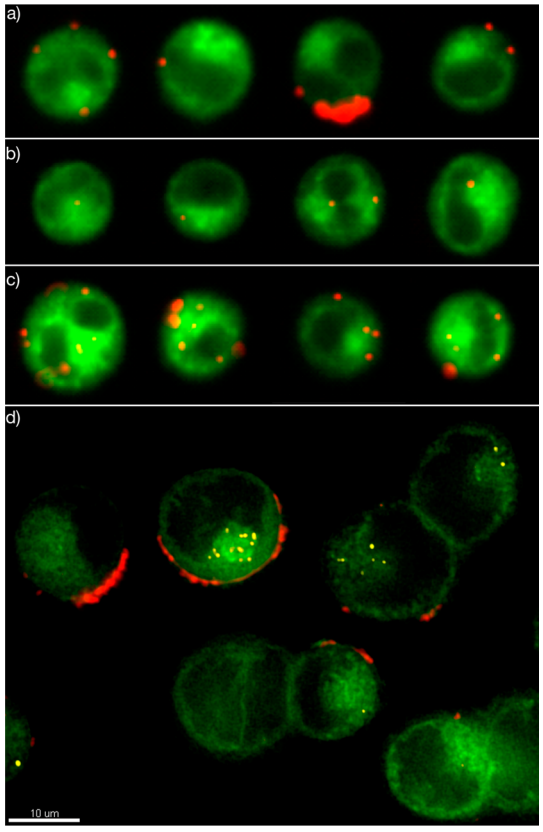

Figure 7. Representative imaging flow cytometry (a−c) and deconvolution microscopy (d) images of huA33 mAb_{Az}-functionalized $PVPON_{Alk}$ capsules (red) incubated with LIM2405+ CRC cells (green) at 37 °C for 4 h. (a) Surface bound capsules. (b) Cells with 1−2 internalized capsules. (c) Cells with multiple internalized capsules. (d) Deconvolution microscopy image to distinguish surface bound capsules (red) from internalized capsules (yellow).

more than one capsule, resulting in an underestimation of the number of internalized capsules (Figure 7a−c). The degree of internalization observed using the imaging flow cytometer was found to be consistent with higher resolution data obtained by using deconvolution microscopy (Figure 7d).

While the percentage of cells containing internalized capsules is markedly higher for cells incubated with huA33 mAb_{Az}-functionalized capsules compared to nontargeted capsules, these data *per se* do not indicate an active role for the huA33 mAb in the internalization process, such as the triggering of receptor-mediated endocytosis. Rather, the huA33 mAb may be playing a more passive role by facilitating the accumulation of capsules on the cell surface. To investigate this, we analyzed the internalization of capsules in subsets of cells that were associated with a capsule on the cell surface (Figure 6b). When LIM2405+ cells are incubated with huA33 mAb_{Az}-functionalized capsules at 4 °C (to prevent internalization), less than 10% of cells contain internalized capsules (Figure 6a,b). This confirms that the image processing by the imaging flow cytometer can successfully distinguish internalized capsules from surface bound capsules. When the temperature is raised to 37 °C to permit internalization, the percentage of cells with internalized capsules is approximately 55−65%, regardless of whether the capsules were functionalized with huA33 mAb_{Az} or IgG or whether the cells express the A33 antigen or not. The number of huA33 mAb_{Az} capsules within the LIM2405+ cells is clearly greater than the number of IgG-functionalized capsules (Figure 6b). This can be attributed to the accumulation of a larger number of capsules on the cell surface, rather than the huA33 mAb triggering a specific receptor-mediated mechanism of internalization. In a previous study, we investigated the internalization of nonfunctionalized capsules prepared from PMA (rather than PVPON) and

determined that unmodified capsules are most likely internalized *via* a nonspecific "cell drinking" mechanism known as macropinocytosis.[22] The Ab-functionalized capsules were found to localize within the acidic lysosomes (data not shown), which is consistent with what we observed in our previous study for nonfunctionalized PMA capsules.[22] Similarly, De Geest and coworkers demonstrated that 3 μm diameter dextran sulfate/poly-L-arginine capsules were internalized into dendritic cells *via* macropinocytosis.[23] This fits in well with the results reported here, whereby targeted capsules accumulate on the surface of cells *via* specific and high affinity antibody−antigen interactions and are then internalized *via* macropinocytosis. Once bound to the cell surface, either specifically in the case of huA33 mAb_{Az}-functionalized capsules or nonspecifically for the IgG and nonfunctionalized capsules, the probability that the capsule will be internalized is similar, regardless of the binding mechanism. This suggests that the huA33 mAb strongly promotes the accumulation of targeted capsules on the surface of cells expressing the A33 antigen, which facilitates their internalization *via* an antibody-independent mechanism.

CONCLUSION

Targeting aberrant cells and understanding how they interact with nanoengineered materials is critical for the development of better treatments for diseases such as cancer. In this study, we have interrogated the interaction of sub-micrometer-sized, low fouling,[14] huA33 mAb_{Az}-functionalized PVPON capsules with human CRC cells. We found that the percentage of cells associated with capsules increases as the capsule-to-cell ratio increases to 100:1, reaching a plateau of 95% at a 600:1 ratio. The number of capsules associated with each cell continues to rise as the capsule-to-cell ratio increases. The density of the huA33 mAb on the surface of the capsules also influences both the percentage of cells with capsules bound and the total number of capsules associated with them. In mixed cell populations, the specific binding of the huA33 mAb_{Az}-functionalized capsules is still effective, even when the target cells are present at less than 0.1% of the total cell population. When incubated with cells at 37 °C for 2 h, significant internalization of the capsules is observed. This internalization is independent of capsule functionalization, suggesting an antibody-independent internalization mechanism, such as macropinocytosis. We anticipate that the results outlined here will have broad applicability for the targeting of a variety of nanoengineered particles, including polymersomes, liposomes, polyion complexes, and inorganic nanoparticles.

EXPERIMENTAL SECTION

Methods. Capsule synthesis,[14] Ab modification,[11] and fluorescence modification of capsules[14] were performed as described previously and are summarized in the Supporting Information.

Functionalization of $PVPON_{Alk}$ Capsules with huA33 mAb. Twenty micrograms of labeled huA33 mAb_{Az} was added to 1.6×10^8 of $PVPON_{Alk}$ capsules in phosphate buffered saline (PBS with 10 μL of 4.4 g L^{-1} sodium ascorbate, 10 μL of 1.8 g L^{-1} copper sulfate, and 10 μL of 4.89 g L^{-1} chelator (tris[(4-carboxyl-1-benzyl-1*H*-1,2,3-triazol-4-yl)methyl]amine) (TCBTMA) (see Figure S1).[24] Samples were incubated with constant shaking for 45 min at 4 °C, and after functionalization, the capsules were washed twice in PBS.

For flow cytometry and fluorescence microscopy measurements to qualitatively verify huA33 mAb conjugation (Figure 1), capsules of ~3.8 μm diameter were used.

Cell Targeting. For flow cytometry experiments, LIM1899 cells were trypsinized followed by incubation with either huA33 mAb_{Az}, IgG-, or nonfunctionalized capsules for 1 h at 4 °C. All capsules were labeled with AF647. The capsule-to-cell ratio was varied from 10:1 to 600:1. After incubation, the cells were washed with PBS at 4 °C and the pellet was resuspended in 1 mL of PBS and analyzed by flow cytometry (Partec Cyflow Space). Analysis of huA33 mAb_{Az} functionalization was performed using FlowJo v8.7 (TreeStar).

Deconvolution Fluorescence Microscopy. Deconvolution fluorescence microscopy was performed on a DeltaVision (Applied Precision) microscope with a 60× 1.42 NA oil objective with a standard FITC/TRITC/CY5 filter set. Images were processed with Imaris (Bitplane) using the maximum intensity projection unless otherwise noted.

Mixed Cell Targeting. LIM2405+ cells were fluorescently labeled with CellTracker CMFDA, and LIM2405− cells were fluorescently labeled with LavaCell according to the distributor's protocol. The labeled LIM2405+ and LIM2405− cells were then mixed together to achieve a 10-, 100-, and 1000-fold excess of LIM2405− cells over LIM2405+ cells, with a total of 200 000 cells per sample. The huA33 $_{Az}$ mAb_{Az}-, IgG-, or nonfunctionalized capsules were then added to the cell mixture and incubated for 1 h at 4 °C prior to flow cytometry analysis (Partec Cyflow Space).

Internalization of Capsules. Pure populations of LIM2405+ and LIM2405− cells (1×10^5 cells per well) were seeded in a 48-well tissue culture plate. Cells were then incubated with either huA33 mAb_{Az}-, IgG-, or nonfunctionalized AF647 capsules at 37 °C for 2 h. The huA33 mAb_{Az}-functionalized capsules were also incubated with LIM2405+ capsules at 4 °C for 2 h to prevent internalization and were used as a control for noninternalized capsules. After 2 h, cells were trypsinized, washed three times in PBS, and analyzed using an imaging flow cytometer (Amnis ImageStream). Images were acquired for 10 000 cells for each sample, and after excluding aggregated and out of focus cells, at least 3000 cells were analyzed.

Conflict of Interest: The authors declare no competing financial interest.

Acknowledgment. This work was supported by the Australian Research Council (ARC) under the Discovery Project (DP0877360), Future Fellowship (FT110100265), and Federation Fellowship (FF0776078) schemes, and by the National Health and Medical Research Council (NHMRC 433607) of Australia Program Grant 487992 and Senior Research Fellowship.

Supporting Information Available: Experimental details for capsules and antibody preparation, and structure of the TCBTMA chelator. This material is available free of charge *via* the Internet at http://pubs.acs.org.

REFERENCES AND NOTES

1. Johnston, A. P. R.; Such, G. K.; Ng, S. L.; Caruso, F. Challenges Facing Colloidal Delivery Systems: From Synthesis to the Clinic. *Curr. Opin. Colloid Interface Sci.* **2011**, *16*, 171–181.

2. van Dongen, S. F. M.; de Hoog, H.-P. M.; Peters, R. J. R. W.; Nallani, M.; Nolte, R. J. M.; van Hest, J. C. M. Biohybrid Polymer Capsules. *Chem. Rev.* **2009**, *109*, 6212–6274.
3. De Koker, S.; De Cock, L. J.; Rivera-Gil, P.; Parak, W. J.; Auzély Velty, R.; Vervaet, C.; Remon, J. P.; Grooten, J.; De Geest, B. G. Polymeric Multilayer Capsules Delivering Biotherapeutics. *Adv. Drug Delivery Rev.* **2011**, *63*, 748–761.
4. Debbage, P. Targeted Drugs and Nanomedicine: Present and Future. *Curr. Pharm. Des.* **2009**, *15*, 153–172.
5. Peer, D.; Karp, J. M.; Hong, S.; Farokhzad, O. C.; Margalit, R.; Langer, R. Nanocarriers as an Emerging Platform for Cancer Therapy. *Nat. Nanotechnol.* **2007**, *2*, 751–760.
6. Shi, M.; Lu, J.; Shoichet, M. S. Organic Nanoscale Drug Carriers Coupled with Ligands for Targeted Drug Delivery in Cancer. *J. Mater. Chem.* **2009**, *19*, 5485–5498.
7. Finn, M.; Sharpless, K. Click Chemistry: Diverse Chemical Function from a Few Good Reactions. *Angew. Chem., Int. Ed.* **2001**, *40*, 2004–2021.
8. Lee, S.-M.; Chen, H.; O'Halloran, T. V.; Nguyenqq, S. T. "Clickable" Polymer-Caged Nanobins as a Modular Drug Delivery Platform. *J. Am. Chem. Soc.* **2009**, *131*, 9311–9320.
9. Kinnane, C. R.; Wark, K.; Such, G. K.; Johnston, A. P. R.; Caruso, F. Peptide-Functionalized, Low-Biofouling Click Multilayers for Promoting Cell Adhesion and Growth. *Small* **2009**, *5*, 444–448.
10. Lu, J.; Shi, M.; Shoichet, M. S. Click Chemistry Functionalized Polymeric Nanoparticles Target Corneal Epithelial Cells through RGD-Cell Surface Receptors. *Bioconjugate Chem.* **2009**, *20*, 87–94.
11. Kamphuis, M. M. J.; Johnston, A. P. R.; Such, G. K.; Dam, H. H.; Evans, R. A.; Scott, A. M.; Nice, E. C.; Heath, J. K.; Caruso, F. Targeting of Cancer Cells Using Click-Functionalized Polymer Capsules. *J. Am. Chem. Soc.* **2010**, *132*, 15881–15883.
12. Elias, D. R.; Cheng, Z.; Tsourkas, A. An Intein-Mediated Site-Specific Click Conjugation Strategy for Improved Tumor Targeting of Nanoparticle Systems. *Small* **2010**, *6*, 2460–2468.
13. Thorek, D. L. J.; Elias, D. R.; Tsourkas, A. Comparative Analysis of Nanoparticle-Antibody Conjugations: Carbodiimide *versus* Click Chemistry. *Mol. Imaging* **2009**, *8*, 221–229.
14. Kinnane, C. R.; Such, G. K.; Antequera-Garcia, G.; Yan, Y.; Dodds, S. J.; Liz-Marzan, L. M.; Caruso, F. Low-Fouling Poly(*N*-vinyl pyrrolidone) Capsules with Engineered Degradable Properties. *Biomacromolecules* **2009**, *10*, 2839–2846.
15. Becker, A. L.; Johnston, A. P. R.; Caruso, F. Layer-by-Layer-Assembled Capsules and Films for Therapeutic Delivery. *Small* **2010**, *6*, 1836–1852.
16. Such, G. K.; Johnston, A. P. R.; Liang, K.; Caruso, F. Synthesis and Functionalization of Nanoengineered Materials Using Click Chemistry. *Prog. Polym. Sci.* **2012**, *37*, 985–1003.
17. Scott, A. M.; Lee, F. T.; Jones, R.; Hopkins, W.; MacGregor, D.; Cebon, J. S.; Hannah, A.; Chong, G.; U, P.; Papenfuss, A. *et al.* A Phase I Trial of Humanized Monoclonal Antibody A33 in Patients with Colorectal Carcinoma: Biodistribution, Pharmacokinetics, and Quantitative Tumor Uptake. *Clin. Cancer Res.* **2005**, *11*, 4810–4817.
18. Johnstone, C.; Tebbutt, N.; Abud, H.; White, S.; Stenvers, K.; Hall, N.; Cody, S.; Whitehead, R.; Catimel, B.; Nice, E.; *et al.* Characterization of Mouse A33 Antigen, a Definitive Marker for Basolateral Surfaces of Intestinal Epithelial Cells. *Am. J. Physiol. Gastrintest. Liver Physiol.* **2000**, *279*, G500–G510.
19. Hong, V.; Steinmetz, N. F.; Mancherster, M.; Finn, M. G. Labeling Live Cells by Copper-Catalyzed Alkyne-Azide Click Chemistry. *Bioconjugate Chem.* **2010**, *21*, 1912–1916.
20. Whitehead, R.; Zhang, H.; Hayward, I. Retention of Tissue-Specific Phenotype in a Panel of Colon Carcinoma Cell Lines: Relationship to Correlates. *Immunol. Cell Biol.* **1992**, *70*, 227–236.
21. Heath, J.; White, S.; Johnstone, C.; Catimel, B.; Simpson, R.; Moritz, R.; Tu, G.; Ji, H.; Whitehead, R.; Groenen, L.; *et al.* The Human A33 Antigen Is a Transmembrane Glycoprotein and a Novel Member of the Immunoglobulin Superfamily. *Proc. Natl. Acad. Sci. U.S.A.* **1997**, *94*, 469–474.
22. Yan, Y.; Johnston, A. P. R.; Dodds, S. J.; Kamphuis, M. M. J.; Ferguson, C.; Parton, R. G.; Nice, E. C.; Heath, J. K.; Caruso, F. Uptake and Intracellular Fate of Disulfide-Bonded Polymer Hydrogel Capsules for Doxorubicin Delivery to Colorectal Cancer Cells. *ACS Nano* **2010**, *4*, 2928–2936.
23. De Koker, S.; De Geest, B. G.; Singh, S. K.; De Rycke, R.; Naessens, T.; Van Kooyk, Y.; Demeester, J.; De Smedt, S. C.; Grooten, J. Polyelectrolyte Microcapsules as Antigen Delivery Vehicles to Dendritic Cells: Uptake, Processing, and Cross-Presentation of Encapsulated Antigens. *Angew. Chem., Int. Ed.* **2009**, *48*, 8485–8489.
24. Hong, V.; Udit, A.; Evans, R.; Finn, M. Electrochemically Protected Copper(I)-Catalyzed Azide–Alkyne Cycloaddition. *ChemBioChem* **2008**, *9*, 1481–1486.